HHS Public Access

Author manuscript

J Am Soc Mass Spectrom. Author manuscript; available in PMC 2023 May 11.

Published in final edited form as:

J Am Soc Mass Spectrom. 2022 November 02; 33(11): 2156–2164. doi:10.1021/jasms.2c00225.

Identification of monomethyl branched chain lipids by a combination of liquid chromatography tandem mass spectrometry and charge-switching chemistries

Caitlin E. Randolph[†], **Connor H. Beveridge**[†], **Sanjay Iyer**[†], **Stephen J. Blanksby**[‡], **Scott A. McLuckey**[†], **Gaurav Chopra**[†,⊥,*]

[†]Department of Chemistry, Purdue University, West Lafayette, Indiana 47907-2084, USA

[‡]Central Analytical Research Facility and the School of Chemistry and Physics, Queensland University of Technology, Brisbane, QLD 4000, Australia

[⊥]Department of Computer Science (by courtesy), Purdue Institutes of Drug Discovery and Integrative Neuroscience, Purdue Center for Cancer Research, West Lafayette, Indiana, 47907, USA

Abstract

While various mass spectrometric approaches have been applied to lipid analysis, unraveling the extensive structural diversity of lipids remains a significant challenge. Notably, these approaches often fail to differentiate between isomeric lipids - a challenge that is particularly acute for branched-chain fatty acids (FAs) that often share similar (or identical) mass spectra to their straight-chain isomers. Here, we utilize charge-switching strategies that combine ligated magnesium dications with deprotonated fatty acid anions. Subsequent activation of these charge inverted anions yields mass spectra that differentiate *anteiso* branched- from straight-chain and *iso* branched-chain FA isomers with the predictable fragmentation enabling *de novo* assignment of *anteiso* branch points. Application of these charge-inversion chemistries in both gas- and solution-phase modalities is demonstrated to assign the position of *anteiso*-methyl branch-points in FAs, and, with the aid of liquid chromatography, can be extended to *de novo* assignment of additional branching sites via predictable fragmentation patterns as methyl branching site(s) move closer to the carboxyl carbon. The gas phase approach is shown to be compatible with top-down structure elucidation of complex lipids such as phosphatidylcholines, while integration of solution-phase charge-inversion with reversed phase liquid chromatography enables separation and unambiguous identification of FA structures within isomeric mixtures. Taken together, the presented charge

[*]Address reprint requests to: Dr. Gaurav Chopra, 560 Oval Drive, Department of Chemistry, Purdue University, West Lafayette, IN 47907-2084, USA, Phone: (765) 496-6108, Fax: (765) 494-0239, gchopra@purdue.edu.

Competing Interests

G.C. is the Director of the Merck-Purdue Center for Measurement Science funded by Merck Sharp & Dohme, a subsidiary of Merck. The remaining authors declare no competing interests.

Associated Content

Supporting Information

Additional information discussed in the text that support the presentation of the work (PDF)

(Figure S1) product ion spectrum resulting from the mutual storage ion/ion reaction between $[FA - H]^-$ anions and $[MgTerpy_2]^{2+}$ reagent cations, (Figure S2) CID spectrum of $[PC\ 16:0/14:0(12Me) + CH_3CO_2]^-$, and (Figure S3) MS/MS spectra of BCFA-MgTerpy complex cations obtained on the triple quadrupole mass spectrometer following condensed-phased charge switch derivatization.

switching MS-based technique, in combination with liquid chromatography enables the structural identification of branched-chain FA without the requirement of authentic methyl branched FA reference standards.

Graphical Abstract

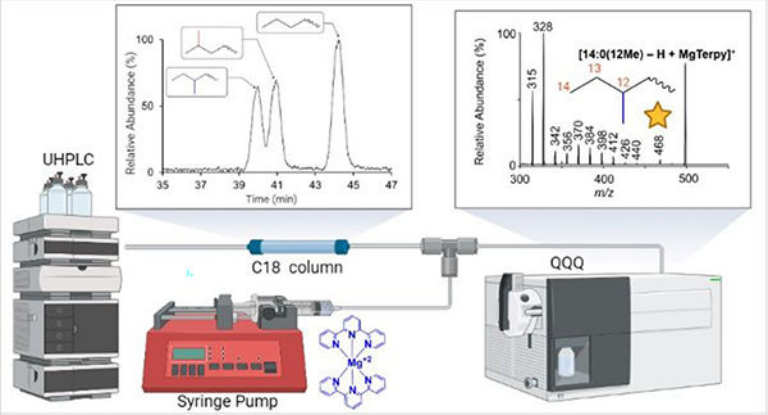

Schematic of post-column charge switching LC-MS/MS method

Introduction

Fatty acids (FAs) constitute an essential lipid class in all living systems, serving pivotal biological roles in various physiological functions and during inflammation, affecting immune response and apoptosis.[1–3] Moreover, FAs are building blocks of many complex lipid structures where they are coupled via an ester, ether, or amide linkage to structural backbones including glycerol, sphingosine and carbohydrates. The general FA structure consists of a carboxylic acid group and a hydrocarbon chain. Variations in carbon-chain length, degree of unsaturation, location and stereochemistry of unsaturation site(s), chain branching, and functionalization (*e.g.*, nitration, hydroxylation, *etc.*) lead to a vast array of potential FA structures. The modification of lipid structure impacts both chemical and physical properties. Furthermore, these structural variations inform the physiological role of individual lipid molecules.[1,4,5] Importantly, recent research implicates alterations in FA structure and/or composition associated with lipid metabolism dysregulation in numerous pathologies, including cancer, cardiovascular diseases, neurodegeneration, and diabetes.[6–13] For example, long-chain saturated fatty acids were identified as the toxic factor killing injured neurons and oligodendrocytes in the brain during inflammation.[14] Consequently, analytical methods capable of accurately identifying and quantifying FAs in complex biological samples are needed in order to unravel their roles in health and disease.

Branched-chain fatty acids (BCFAs) are a unique structural subset of the fatty acyl lipid class. BCFAs are known to dominate many bacterial lipid profiles.[15–20] For example, BCFAs have been suggested to constitute more than 75% of the total fatty acid profile of *Bacillus subtilis.*[20,15] While BCFAs are minor lipid components of internal mammalian tissues, they have been detected as major components of meibomian gland secretions (within the eyelid) and vernix caseosa, the sebaceous wax coating human newborns.[21–23]

Specific short BCFAs, such as valproic acid are used as a mood-stabilizing and anti-epileptic drug but also cause neurotoxic effects and anti-convulsant effects related to neural tube defects, congenital defects and fetal growth.[24–28] Among the most common BCFAs are saturated FAs with a methyl group at either the antepenultimate or penultimate carbon, known as the *anteiso*- or *iso*-position, respectively. Traditionally, gas chromatography-mass spectrometry (GC-MS) is deployed to resolve BCFAs from their straight-chain isomers and to facilitate identification and quantitation in complex biological samples.[1,18,29–31] In general, GC-MS analysis first requires the conversion of FA structures to fatty acid methyl esters (FAMEs) to increase analyte volatility. Unfortunately, branched-chain fatty acid methyl esters (BCFAMEs) often co-elute with other FAMEs, even with the use of long, highly-polar columns.[31] The problem of resolution and unambiguous identification is further compounded by high degree of similarity in the conventional (70 eV) electron ionization (EI) mass spectra of isomeric FAMEs. Thus, the presence of structurally distinct FAs can be masked in both chromatographic and mass spectrometric dimensions that further hinders the detection, identification, and quantitation of BCFAs. Moreover, BCFAME identification is often accomplished using spectral matching or via the use of retention time alignment, both of which require the utilization of reference standards that are often costly and rarely available. To circumvent these issues, Murphy and co-workers combined electron-ionization with collision-induced dissociation demonstrating that activation of the molecular ions of FAMEs gives rise to mass spectra that were much more sensitive to molecular structure; including the position(s) of methyl-chain branching.[32] Brenna and co-workers have utilized this approach to provide detailed structure elucidation of branched-chain fatty acids in lipid extracts from human cell lines and food.[18,31] Notably, this approach enables the mass spectrometric resolution of co-eluting GC peaks and is thus capable of both quantitative and qualitative analyses of BCFAMEs without reference standards. One challenge with this approach is that the molecular ion abundance resulting from EI of FAMEs is low and can impact sensitivity. Alternative GC-MS approaches that can increase the sensitivity for detection and identification of BCFAs rely upon wet-chemical derivatization strategies prior to analysis that are designed to promote sensitive detection and structurally diagnostic fragmentation upon EI. Two of the most successful and widely adopted examples include 4,4-dimethyloxazoline (DMOX) and 3-pyridylcarbinol (historically –and incorrectly– referenced as ‘picolinyl’) ester derivatives of FAs.[29,33–35] Both derivatives produce EI mass spectra with fragmentation patterns that can identify structural motifs including branching points in the acyl chain. Both methods require offline wet-chemical preparation prior to GCMS. However, complex lipid hydrolysis of fatty acyl chains from complex lipid precursors results in the loss of valuable information regarding origin and function of BCFAs.

Due to recent advances in electrospray-ionization mass spectrometry (ESI-MS) and liquid chromatography (LC) protocols, LC-MS is gaining wider acceptance as an alternative approach to the identification and quantification of FAs in biological extracts.[1,10,14,36,37] In these protocols, free FA (or those liberated by hydrolysis) can be subjected to LC-MS directly or analysis of complex lipids can be analyzed by LC-MS with subsequent interrogation of the FA building blocks enabled by fragmentation of the precursor lipid in tandem mass spectrometry (MS/MS) modalities. When subjected to conventional low

energy collision-induced dissociation (CID), singly deprotonated FA anions (denoted $[FA - H]^-$ and formed directly or as fragmentation products ions from complex lipids) typically results in very little fragmentation from dissociation of the carbon–carbon bonds in the acyl chain, as the dominant product ions observed correspond to decarboxylation ($-CO_2$) and dehydration ($-7H_2O$) of the FA precursor anion.[38,39] To increase the generation of structurally informative product ions, charge-inversion of FAs has been explored, often in concert with novel laser-based dissociation strategies like photodissociation (PD) and ultraviolet photodissociation (UVPD).[40–45] Extending the radical-directed dissociation approaches for complex lipids developed by the Julian and Blanksby groups, the Xia group has identified the location(s) of methyl branching in bacterial glycerophospholipids, including sphingomyelins, phosphatidylcholines, and phosphatidylethanolamines.[42,46–49] Recently, we have described the efficacy of gas-phase ion/ion charge inversion reactions for the identification of FA both in non-esterified forms and also when esterified within complex lipids.[50–57] This strategy has significant advantages as it can exploit the preferred ionization and fragmentation of many lipids in negative ion mode while taking advantage of structurally-selective charge-remote fragmentation in charge-inverted positive ions. Herein, we demonstrate the ability of charge-inversion ion/ion reactions combined with CID to differentiate isomeric BCFAs. Additionally, we present the development of a LC-MS/MS method that deploys post-column charge-switch derivatization to provide online and unambiguous discrimination of (1) non-branched and branched acyl chains from isomeric methyl branched lipid structures and (2) the identification of methyl chain branching site in saturated BCFAs.

Experimental

Nomenclature

Here, we adopt the shorthand notation recommended by Liebisch et al.[58] Briefly, fatty acyl chains are described by the total number of carbons, as indicated before the colon, and the total number of double bonds, as indicated after the colon. When present, the methyl branch functional group is abbreviated as “Me”. Identified positions of methyl branching are shown within parenthesis after the integer indicating the number of double bonds. For example, 13-methlytetradecanoic acid, commonly referred to as isopentadecylic acid (*iso* 15:0), can be represented as FA 14:0(13Me). Similarly, 12-methlytetradecanoic acid, commonly referred to as anteisopentadecylic acid (*anteiso* 15:0), can be represented as FA 14:0(12Me).

Materials

HPLC-grade methanol, water, and acetic acid solution were purchased from Fisher Scientific (Pittsburgh, PA). Magnesium chloride and 2 2′:6′,2″-(Terpy) purchased from Millipore-Sigma (St. Louis, MO). The following lipid standards were purchased from Avanti Polar Lipids, Inc. (Alabaster, AL): 12-methlytetradecanoic acid (FA 14:0(12Me) or *anteiso* 15:0), 13-methlytetradecanoic acid (FA 14:0(13Me) or *iso* 15:0), 1-palmitoyl-(12S-methylmyristoyl)-sn-glycero-3-phosphocholine (PC 16:0/*anteiso* 15:0 or PC 16:0/14:0(12Me)), 1-palmitoyl-(13S-methylmyristoyl)-sn-glycero-3-phosphocholine (PC

16:0/*iso* 15:0 or PC 16:0/14:0(13Me)). Pentadecanoic acid (FA 15:0) was purchased from Cayman Chemical (Ann Arbor, MI).

Gas phase ion/ion experiments

All gas-phase charge inversion data were collected on a Sciex QTRAP 4000 hybrid triple quadrupole/linear ion trap mass spectrometer (SCIEX, Concord, ON, Canada) with modifications analogous to those previously described.[59] Alternately, pulsed nano-electrospray ionization (nESI) allows for sequential injection of lipid anions and charge inversion reagent bis-terpyridine magnesium dications, $[MgTerpy_2]^{2+}$.[60] Mass spectra were produced via the analysis of ions using mass-selective axial ejection (MSAE).[61]

Scheme 1 illustrates the generation of $[FA - H + MgTerpy]^+$ complex cations. Briefly, singly deprotonated FA anions are transformed via gas-phase ion/ion reaction with bis-terpyridine magnesium dications. First, $[FA - H]^-$ were generated via direct negative nESI of either (1) a methanolic solution of fatty acid standard or (2) from the liberation fatty acyl carboxylate anions from a phospholipid precursor anion utilizing collisional activation of lipid anions in q2 via single frequency resonance excitation which results in the cleavage of *sn*-1 and *sn*-2 ester bonds and production of singly deprotonated FA anions.[52] Following the generation of $[FA - H]^-$ anions, reagent dications were mass-selected during transit through Q1 and transferred to q2. Together in q2, reagent $[MgTerpy_2]^{2+}$ dications and $[FA - H]^-$ anions were permitted to react, yielding charge-inverted $[FA - H + MgTerpy]^{2+}$ complex cations. Next, monoisotopic isolation and ion trap CID of charge-inverted FA complex cations permit unambiguous isomeric *anteiso* branched- and straight-chain lipid discrimination via exploitation of reproducible spectral patterns.

LC-MS/MS experiments

Lipid samples dissolved in methanol at ~ 1 μM were placed in the autosampler of an Agilent 1290 Infinity II LC System (Santa Clara, CA). 1 μL of lipid solution was injected onto an Ascentis® Express C18-HPLC column (150 × 3 mm, 2.7 X(8 at 25°C. The mobile phase A was methanol, and mobile phase B was 97/3 Water/MeOH with 15 mM acetic acid (v/v). To achieve separation, a gradient beginning with 80% B and increasing to 88% B over 73 minutes at a flow rate of 0.2 mL min^{-1} was used. At 74 mins, the mobile phase composition was returned to and held at initial conditions for a total of 11 mins to re-equilibrate the column. The total run time was 85 mins. The post-column eluent was combined with a methanolic solution of $[MgTerpy_2]^{2+}$ (100 μM) via a syringe pump and T-junction prior to infusion into the mass spectrometer to facilitate the formation of $[FA - H + MgTerpy]^+$ cations. To make the solution of $[MgTerpy_2]^{2+}$, equimolar amounts of magnesium chloride and 2,2′:6′2″-terpyridene were first combined and dissolved in methanol, before dilution prior to analysis.

Mass spectra were recorded using an Agilent 6495C triple quadrupole mass spectrometer (Santa Clara, CA) equipped with a Jet Stream ESI source. All mass spectra reported here are the result of 30–50 scan averages. The instrument was operated in positive ion mode. Product ion scans were collected using a normalized collision energy (CE) of 55 eV. Nitrogen served as the sheath, drying, and collision gases. MS parameters were optimized

and set as: drying gas temperature at 150°C, dry gas flow rate at 15 L min^{-1}, sheath gas temperature at 225°C, sheath gas flow rate at 11 L min^{-1}, nebulizer pressure at 30 psi, capillary voltage at 3500 V, and nozzle voltage at 1500 V.

Results and Discussion

Saturated straight-chain and branched lipid analysis using ion/ion chemistry.

Saturated and branched FA anions undergo charge inversion when subjected to mutual storage with $[MgTerpy_2]^{2+}$ reagent dications in the high-pressure collision cell q2. As a result of the ion/ion reaction, singly deprotonated FA anions are transformed to [FA − H + MgTerpy]$^+$ cations (Supporting Information Figure S1). Figure 1 shows the ion trap CID spectra of a series of [FA − H + MgTerpy]$^+$ ions derived from straight chain FA 15:0 and two branched-chain variants, 13-methyltetradecanoic acid (FA 14:0(13Me)) and 12-methyltetradecanoic acid (FA 14:0(12Me)). The CID spectrum of [FA 15:0 − H + MgTerpy]$^+$ displays an uninterrupted series of product ions between *m/z* 315 and 468 with 14 Da spacings, noting that product ion relative abundance generally decreases as carbon-carbon fragmentation approaches the methyl end of aliphatic chain (Figure 1A). Collisional activation of the charge-inverted FA 14:0(12Me) ion, as shown in Figure 1B, contains a series of product ions spaced at 14 Da apart and generated via carbon-carbon bond cleavage beginning at C2-C3 (*m/z* 315) and ending at C12-C13 (*m/z* 468). Importantly, as fragmentation approaches the methyl branching site, a dramatic suppression in product ion relative abundance is observed, as highlighted with the low abundance product ion observed at *m/z* 454. Flanking the methyl branching site, carbon-carbon bond cleavage generates more highly abundant product ions, as indicated with the product ions observed at *m/z* 440 and *m/z* 468 (Figure 1B). In comparison, Figure 1C displays the CID spectrum of [FA 14:0(13Me) − H + MgTerpy]$^+$. Notably absent in the product ion spectrum of the charge inverted FA 14:0(13Me) ion is an abundant product ion at *m/z* 468. However, the product ion spectra of [FA 14:0(13Me) − H + MgTerpy]$^+$ (Figure 1C) and [FA 15:0 − H + MgTerpy]$^+$ (Figure 1A) are nearly identical, with only subtle differences in relative product ion abundances observed. Thus, the *anteiso* isomer can be distinguished from straight-chain and *iso* isomers, but the latter cannot be distinguished from each other. Therefore, other methods must be used to distinguish the latter two isomers.

The development of a top-down shotgun-MS method utilizing gas phase ion/ion charge inversion chemistry provides near-complete glycerophospholipid (GPL) structural identification as described previously.[52] To date, few approaches are capable of discerning methyl-branching site in complex lipid structures. We report an MS^n experiment involving ion/ion chemistry to facilitate the assignment of the GPL headgroup and fatty acyl composition, identification of the presence of *anteiso* methyl branching position in saturated acyl chains, and, in some cases, assignment of fatty acyl *sn*-position. To demonstrate this approach, we examined synthetic phosphatidylcholines (PCs), including PC 16:0/14:0(12Me) and PC 16:0/14:0(13Me). Briefly, as ionization of PCs in negative ion mode relies on the formation of an adduct ion (*e.g.*, $[M + X]^-$ where X = Cl or CH_3CO_2), direct negative nESI of PC 16:0/14:0(12Me) resulted in the generation of abundant [PC + $CH_3CO_2]^-$ precursor anions. Next, CID of mass-selected [PC 16:0/14:0(12Me) + $CH_3CO_2]^-$

(*m/z* 778) generated demethylated PC product anions (*i.e.*, [PC 16:0/14:0(12Me) − CH_3]$^-$) detected at *m/z* 704. The product ion spectrum of [PC 16:0/14:0(12Me) + CH_3CO_2]$^-$ (*m/z* 778) displayed in Figure S2 ultimately permits identification of the polar headgroup. To release FA anions from the GPL precursors, subsequent ion-trap CID of the [PC 16:0/14:0(12Me) − CH_3]$^-$ was employed, as detailed in Figure 2A. The greater abundance of the *sn*-2 [14:0(12Me) − H]$^-$ fragment ion (*m/z* 241) relative to the *sn*-1 [16:0 − H]$^-$ (*m/z* 255) is in good agreement with previous observations, and suggests preferential formation of the carboxylate anion from the *sn*-2 acyl substituent.[62] Importantly for unknown lipids, fatty acyl chain regiochemical assignments based only on relative abundances of the carboxylate anions alone are insufficient without calibrating to standards and should be made with caution.[63] However, it can provide a useful guide to the dominant regiochemistry *i.e.* the most abundant regioisomer.

To generate charge-inverted FA complex cations, all MS^3 product ions, including [FA − H]$^-$ anions, were allowed to react with [$MgTerpy_2$]$^{2+}$ dications. The ion/ion reaction mostly resulted in the formation of [FA − H + MgTerpy]$^+$ complex cations (Figure 2B). Subsequent interrogation of the charge-inverted 14:0(12Me) complex cation permits the unambiguous assignment of methyl branching site in an the same fashion as described above (Figure 2C). Employing an identical MS^n and ion/ion approach, isomeric PC 16:0/14:0(13Me) was examined, noting that the MS^2, MS^3, and ion/ion product ion spectra are identical to those described for PC 16:0/14:0(12Me). However, in the case of PC 16:0/14:0(13Me), collisional activation of the MgTerpy derivative of FA 14:0(13Me) generates a CID spectrum distinguishable from that of FA 14:0(12Me) derived from PC 16:0/14:0(12Me) (*c.f.* Figure 2C and 2D). Importantly, the CID spectra of charge-inverted branched FAs derived from non-esterified FAs or from complex GPL precursor anions are identical, meaning that this workflow can be utilized to examine a diverse range of branched lipid species. Moreover, as all GPL classes can be ionized in negative ion mode, fatty acyl anions can be liberated from any GPL precursor anion regardless of headgroup composition using low-energy CID. Thus, the developed gas-phase ion/ion chemistry can be applied to unravel GPL structure, including methyl branching position, independent of the polar headgroup present, further highlighting the versatility of ion/ion platforms.

Charge-switching and LC-MS/MS of synthetic branched fatty acids.

While effective, the inherent complexity of the cellular lipidome can complicate lipid identification, especially when utilizing a shotgun approach, as multiple isomers can be present in a single sample. Moreover, the extensive fragmentation pattern observed upon CID of charge-switched F As only further complicates accurate identification, particularly in the case of complex mixture analysis. While the ion/ion approach described above can confidently distinguish *anteiso* and *iso* branched lipid isomers, this approach is useful only when the straight-chain isomer is not present. As the CID spectra of charge-switched *iso* and straight-chain lipid isomers are nearly identical, structural assignments in the absence of an *anteiso* branched lipid isomer can be ambiguous. To circumvent the shortcomings of the shotgun ion/ion approach, an alternate LC-MS/MS strategy utilizing post-column wet-chemical charge switch derivatization was developed. Importantly, the presented LC-MS/MS charge switching strategy not only enhances mixture analysis performance, but also

eliminates ambiguities in the assignment of isomeric saturated FA structures. Specifically, this platform includes reversed phase liquid chromatography (RPLC) interfaced with a commercially available triple quadrupole mass spectrometer. The experimental set up is depicted in Figure 3A. As a first step, $[FA - H + MgTerpy]^+$ complex cations were first generated in solution. To do so, $MgCl_2$, 2,2′:2″-Terpyridine, and a synthetic FA standard were combined in a methanolic solution at room temperature. Next, the methanolic solution was infused directly into the mass spectrometer. Upon ESI, abundant charge-switched FA anions were observed. Notably, the MS/MS spectra of $[14:0(12Me) - H + MgTerpy]^+$ (*m/z* 498) and $[14:0(13Me) - H + MgTerpy]^+$ (*m/z* 498) obtained on the triple quadrupole mass spectrometer following condensed-phased FA derivatization (Figure S3) are identical to those obtained utilizing the gas-phase ion/ion approach described previously for non-esterified FA structures.

Chromatography coupled with mass spectrometry is a well-established means of overcoming the associated challenges with shotgun-MS experiments, providing improved resolution of molecular species. In our approach, the lipid sample was first separated by RPLC. Using a C18 column with the above-described gradient (see LC-MS/MS experiments), a synthetic standard of 14:0(12Me) eluted *ca.* 1 min earlier than isomeric 14:0(13Me), as shown in Figure 3B. Importantly, excellent chromatographic resolution of straight chain FA 15:0 from the two branched-chain variants was achieved, as FA 15:0 eluted nearly 3 min after isomeric 14:0(13Me) (Figure 3B). Although branched-chain FAs are known to elute earlier than their straight-chain isomers on reversed-phase columns, the elution order may not be sufficient for structural assignment in a complex mixture, especially if unknown branched-points are present. As described before, the MS/MS spectra of underivatized (*i.e.*, singly deprotonated FA anions) saturated and branched FA isomers are identical, leading to ambiguous FA identification in the absence of authentic reference standards.

In turn, post-column charge switch derivatization was utilized to enhance structural information obtained from fragmentation experiments. Briefly, the introduction of bis-terpyridine magnesium complex dications as the derivatization reagent via a post-column tee injunction (Figure 3A) facilitated the formation of charge-switched $[FA - H + MgTerpy]^+$ ions from chromatographically resolved FA structures. The extracted ion chromatograms (EICs) of the charge-switched FA products (*m/z* 498) in Figure 3C denote that the slight shift in retention time (*c.f.* Figures 3B and 3C) is attributed to the increase in dead time associated with the tee junction setup. Figure 3C displays three abundant peaks, corresponding to the charge switched post-column derivatization FA products. The first two eluting analytes correspond to the charge-switched FA 14:0(12Me) (RT = 40.0 min) and 14:0(13Me) (RT = 41.0 min) products. Last to elute is the straight-chain FA 15:0 (RT = 44.3 min). Based on these results, methyl branched FA isomers can be distinguished from not only each other but also their straight-chain counterparts based on retention time.

The LC-MS/MS spectra of post-column derivatized FAs 15:0, 14:0(12Me), and 14:0(13Me) are shown in Figure 4 and display key diagnostic fragmentation patterns analogous to those described before utilizing the gas-phase ion/ion approach. Specifically, the product ion observed at *m/z* 468 serves as a diagnostic signature of *anteiso-methyl* chain branching. The indicator product ion at *m/z* 468 is readily observed in the LC-MS/MS spectrum of

charge-switched FA 14:0(12Me), as shown with Figure 4A, and is notably suppressed in the LC-MS/MS spectra of charge-switched FA 14:0(13Me) (Figure 4B) and FA 15:0 (Figure 4C) structures respectively. We note that, while the product ion spectra of the saturated straight chain FA 15:0 and iso-branched FA 14:0(13Me) are nearly identical, excellent chromatographic separation of these isomers prior to MS/MS affords unambiguous FA identification via retention time matching utilizing authentic straight-chain FA reference standards which are readily available from a surplus of commercial vendors. Therefore, the combination of LC and post-column charge switch Derivatization can readly distinguish straight chain and methyl branched FA isomers with detailed structural information of methyl branching sites for respective FA structure. Laslty, noting that fragmentation patterns observed utilizing the presented online LC charge-switching approach are predictable, reproducible, and dependent on saturated FA structure, methyl braching assignments could be made alogorithmically, supporting high-throughput FA identification.

Conclusions

We have demonstrated two separate charge switching approaches for the detailed structural identification of BCFAs. The first approach utilizes an entirely gas-phase strategy in which FA anions are transformed via charge inversion ion/ion reactions with magnesium bis-terpyridine reagent dications, yielding abundant $[FA - H + MgTerpy]^+$ complex cations. Upon collisional activation, charge inverted BCFA complex cations fragment provide distinct diagnostic product ions indicative of methyl chain branching site. Importantly, the presented MS^n gas-phase charge inversion strategy can readily be extended to identify methyl chain branching site on saturated fatty acyl chains esterified in glycerophospholipid structures. However, for shotgun approaches, the existence of multiple isomeric species within a complex mixture may become problematic and hinder accurate BCFA identification. In addition, the gas-phase ion/ion reactions require specialized instrument modifications and highly trained personnel to conduct these analyses. Thus, to improve isomeric mixture analysis performance and ease of use, an LC-MS/MS method employing post-column charge switching derivatization was established based on conventional LC and MS platforms. In this approach, BCFA isomers are effectively separated from each other and from their straight-chain counterparts. Excellent chromatographic resolution alone affords the accurate identification of saturated FA isomers based on retention time matching with authentic reference standards. However, given that several BCFA reference standards are not readily or commercially available, post-column charge switch derivatization facilitated by a continual infusion of magnesium bis-terpyridine reagent solution and subsequent MS/MS affords facile identification of methyl branching site by exploiting the generation of significant indicator product ions influenced by acyl chain branching. Consequently, post-column generation of MgTerpy-adducted FAs permits the localization of methyl chain branching site in the absence of authentic reference standards. The analysis of intact methyl branched complex lipids could not be achieved using this configuration, as it would first require condensed-phase hydrolysis of ester bonds linking acyl chains to the glycerol backbone of complex lipids and subsequent loss of information on the intact structure.

LC-based separations of branched-chain and straight chain isomers of complex lipids have been demonstrated using long gradients.[64] Future efforts will focus on combining such LC

methodologies with ion/ion chemistries for near-complete structure elucidation of complex lipids with branched chain structures. Developing a chemical conjugation toolbox combined with LC-MS/MS promises to empower further discovery of structural complexity within the lipidome.

Supplementary Material

Refer to Web version on PubMed Central for supplementary material.

Acknowledgements

This work was supported, in part, by the NSF I/UCRC Center for Bioanalytical Metrology (Award 1916991), the United States Department of Defense USAMRAA award W81XWH2010665 through the Peer Reviewed Alzheimer's Research Program, the National Institutes of Health (NIH) award, MH R01–128866 by National Institute of Mental Health, and NIH National Center for Advancing Translational Sciences ASPIRE awards to G.C. We would also like to thank Dr. Shane Tichy for his support and Agilent Technologies Inc. for the donation of the Triple Quadrupole LC/MS instrument to Chopra Laboratory. S.A.M. acknowledges funding by the NIH awards, GM R37–45372 and GM R01–118484. S.J.B. acknowledges project funding through the Discovery Program (DP190101486) Australian Research Council (ARC) and the Centre for Materials Science (QUT, Linkage Spark program). The Purdue University Center for Cancer Research funded by NIH grant P30 CA023168 is also acknowledged. The content is solely the responsibility of the authors and does not necessarily represent the official views of the National Institutes of Health.

References

(1). Blanksby SJ; Mitchell TW Advances in Mass Spectrometry for Lipidomics. Annu. Rev. Anal. Chem. 2010, 3 (1), 433–465. 10.1146/annurev.anchem.111808.073705.

(2). Quehenberger O; Armando AM; Brown AH; Milne SB; Myers DS; Merrill AH; Bandyopadhyay S; Jones KN; Kelly S; Shaner RL; Sullards CM; Wang E; Murphy RC; Barkley RM; Leiker TJ; Raetz CRH; Guan Z; Laird GM; Six DA; Russell DW; McDonald JG; Subramaniam S; Fahy E; Dennis EA Lipidomics Reveals a Remarkable Diversity of Lipids in Human Plasma. J. Lipid Res. 2010, 51 (11), 3299–3305. 10.1194/jlr.M009449. [PubMed: 20671299]

(3). Ivanova PT; Milne SB; Myers DS; Brown HA Lipidomics: A Mass Spectrometry Based Systems Level Analysis of Cellular Lipids. Curr. Opin. Chem. Biol. 2009, 13 (5), 526–531. 10.1016/j.cbpa.2009.08.011. [PubMed: 19744877]

(4). Bolla JR; Agasid MT; Mehmood S; Robinson CV Membrane Protein–Lipid Interactions Probed Using Mass Spectrometry. Annu. Rev. Biochem. 2019, 88 (1), 85–111. 10.1146/annurev-biochem-013118-111508. [PubMed: 30901263]

(5). Barrera NP; Zhou M; Robinson CV The Role of Lipids in Defining Membrane Protein Interactions: Insights from Mass Spectrometry. Trends Cell Biol. 2013, 23 (1), 1–8. 10.1016/j.tcb.2012.08.007. [PubMed: 22980035]

(6). Pakiet A; Kobiela J; Stepnowski P; Sledzinski T; Mika A Changes in Lipids Composition and Metabolism in Colorectal Cancer: A Review. Lipids Health Dis. 2019, 18 (1), 29. 10.1186/s12944-019-0977-8. [PubMed: 30684960]

(7). Mesa-Herrera F; Taoro-González L; Valdés-Baizabal C; Diaz M; Marín R Lipid and Lipid Raft Alteration in Aging and Neurodegenerative Diseases: A Window for the Development of New Biomarkers. Int. J. Mol. Sci. 2019, 20 (15), 3810. 10.3390/ijms20153810. [PubMed: 31382686]

(8). Hinterwirth H; Stegemann C; Mayr M Lipidomics: Quest for Molecular Lipid Biomarkers in Cardiovascular Disease. Circ. Cardiovasc. Genet. 2014, 7 (6), 941–954. 10.1161/CIRCGENETICS.114.000550. [PubMed: 25516624]

(9). Butler LM; Perone Y; Dehairs J; Lupien LE; de Laat V; Talebi A; Loda M; Kinlaw WB; Swinnen JV Lipids and Cancer: Emerging Roles in Pathogenesis, Diagnosis and Therapeutic Intervention. Adv. Drug Deliv. Rev. 2020, 159, 245–293. 10.1016/j.addr.2020.07.013. [PubMed: 32711004]

(10). Han X Multi-Dimensional Mass Spectrometry-Based Shotgun Lipidomics and the Altered Lipids at the Mild Cognitive Impairment Stage of Alzheimer's Disease. Biochim. Biophys. Acta BBA - Mol. Cell Biol. Lipids 2010, 1801 (8), 774–783. 10.1016/j.bbalip.2010.01.010.

(11). Gross RW; Han X Shotgun Lipidomics of Neutral Lipids as an Enabling Technology for Elucidation of Lipid-Related Diseases. Am. J. Physiol.-Endocrinol. Metab 2009, 297 (2), E297–E303. 10.1152/ajpendo.90970.2008. [PubMed: 19126783]

(12). Watson AD Thematic Review Series: Systems Biology Approaches to Metabolic and Cardiovascular Disorders. Lipidomics: A Global Approach to Lipid Analysis in Biological Systems. J. Lipid Res. 2006, 47 (10), 2101–2111. 10.1194/jlr.R600022-JLR200. [PubMed: 16902246]

(13). Young RSE; Bowman AP; Tousignant KD; Poad BLJ; Gunter JH; Philp LK; Nelson CC; Ellis SR; Heeren RMA; Sadowski MC; Blanksby SJ Isomeric Lipid Signatures Reveal Compartmentalized Fatty Acid Metabolism in Cancer. J. Lipid Res. 2022, 63 (6), 100223. 10.1016/j.jlr.2022.100223. [PubMed: 35537528]

(14). Guttenplan KA; Weigel MK; Prakash P; Wijewardhane PR; Hasel P; Rufen-Blanchette U; Münch AE; Blum JA; Fine J; Neal MC; Bruce KD; Gitler AD; Chopra G; Liddelow SA; Barres BA Neurotoxic Reactive Astrocytes Induce Cell Death via Saturated Lipids. Nature 2021, 599 (7883), 102–107. 10.1038/s41586-021-03960-y. [PubMed: 34616039]

(15). Bishop DG; Rutberg L; Samuelsson B The Chemical Composition of the Cytoplasmic Membrane of Bacillus Subtilis. Eur. J. Biochem. 1967, 2 (4), 448–453. 10.1111/j.1432-1033.1967.tb00158.x. [PubMed: 4295208]

(16). Kaneda T Iso- and Anteiso-Fatty Acids in Bacteria: Biosynthesis, Function, and Taxonomic Significance. Microbiol. Rev. 1991, 55 (2), 288–302. [PubMed: 1886522]

(17). Kniazeva M; Crawford QT; Seiber M; Wang C-Y; Han M Monomethyl Branched-Chain Fatty Acids Play an Essential Role in Caenorhabditis Elegans Development. PLoS Biol. 2004, 2 (9), e257. 10.1371/journal.pbio.0020257. [PubMed: 15340492]

(18). Wang Z; Wang DH; Park HG; Tobias HJ; Kothapalli KSD; Brenna JT Structural Identification of Monounsaturated Branched Chain Fatty Acid Methyl Esters by Combination of Electron Ionization and Covalent Adduct Chemical Ionization Tandem Mass Spectrometry. Anal. Chem. 2019, 91 (23), 15147–15154. 10.1021/acs.analchem.9b03912. [PubMed: 31689070]

(19). Mostofian B; Zhuang T; Cheng X; Nickels JD Branched-Chain Fatty Acid Content Modulates Structure, Fluidity, and Phase in Model Microbial Cell Membranes. J. Phys. Chem. B 2019, 123 (27), 5814–5821. 10.1021/acs.jpcb.9b04326. [PubMed: 31251616]

(20). Nickels JD; Chatterjee S; Mostofian B; Stanley CB; Ohl M; Zolnierczuk P; Schulz R; Myles DAA; Standaert RF; Elkins JG; Cheng X; Katsaras J *Bacillus Subtilis* Lipid Extract, A Branched-Chain Fatty Acid Model Membrane. J. Phys. Chem. Lett 2017, 8 (17), 4214–4217. 10.1021/acs.jpclett.7b01877. [PubMed: 28825491]

(21). Souchier M; Joffre C; Beynat J; Grégoire S; Acar N; Bretillon L; Bron AM; Bourcier T; Speeg-Schatz C; Creuzot-Garcher C Changes in Meibomian Fatty Acids and Ocular Surface in Patients With Meibomian Gland Dysfunction After Minocycline Treatment. Invest. Ophthalmol. Vis. Sci. 2008, 49 (13), 2391.

(22). Ran-Ressler RR; Devapatla S; Lawrence P; Brenna JT Branched Chain Fatty Acids Are Constituents of the Normal Healthy Newborn Gastrointestinal Tract. Pediatr. Res. 2008, 64 (6), 605–609. 10.1203/PDR.0b013e318184d2e6. [PubMed: 18614964]

(23). Borchman D; Ramasubramanian A Human Meibum Chain Branching Variability with Age, Gender and Meibomian Gland Dysfunction. Ocul. Surf 2019, 17 (2), 327–335. 10.1016/j.jtos.2018.12.005. [PubMed: 30553000]

(24). Nanau RM; Neuman MG Adverse Drug Reactions Induced by Valproic Acid. Clin. Biochem. 2013, 46 (15), 1323–1338. 10.1016/j.clinbiochem.2013.06.012. [PubMed: 23792104]

(25). Chaudhary S; Parvez S An in Vitro Approach to Assess the Neurotoxicity of Valproic Acid-Induced Oxidative Stress in Cerebellum and Cerebral Cortex of Young Rats. Neuroscience 2012, 225, 258–268. 10.1016/j.neuroscience.2012.08.060. [PubMed: 22960313]

(26). Tong V; Teng XW; Chang TKH; Abbott FS Valproic Acid I: Time Course of Lipid Peroxidation Biomarkers, Liver Toxicity, and Valproic Acid Metabolite Levels in Rats. Toxicol. Sci. 2005, 86 (2), 427–435. 10.1093/toxsci/kfi184. [PubMed: 15858223]

(27). Gezginci-Oktayoglu S; Turkyilmaz IB; Ercin M; Yanardag R; Bolkent S Vitamin U Has a Protective Effect on Valproic Acid-Induced Renal Damage Due to Its Anti-Oxidant, Anti-Inflammatory, and Anti-Fibrotic Properties. Protoplasma 2016, 253 (1), 127–135. 10.1007/s00709-015-0796-3. [PubMed: 25802006]

(28). Li X-N; Shu Q; Su JM-F; Perlaky L; Blaney SM; Lau CC Valproic Acid Induces Growth Arrest, Apoptosis, and Senescence in Medulloblastomas by Increasing Histone Hyperacetylation and Regulating Expression of P21Cip1, CDK4, and CMYC. Mol. Cancer Ther. 2005, 4 (12), 1912–1922. 10.1158/1535-7163.MCT-05-0184. [PubMed: 16373706]

(29). Chiu H-H; Kuo C-H Gas Chromatography-Mass Spectrometry-Based Analytical Strategies for Fatty Acid Analysis in Biological Samples. J. Food Drug Anal. 2020, 28 (1), 60–73. 10.1016/j.jfda.2019.10.003. [PubMed: 31883609]

(30). He L; Prodhan MAI; Yuan F; Yin X; Lorkiewicz PK; Wei X; Feng W; McClain C; Zhang X Simultaneous Quantification of Straight-Chain and Branched-Chain Short Chain Fatty Acids by Gas Chromatography Mass Spectrometry. J. Chromatogr. B 2018, 1092, 359–367. 10.1016/j.jchromb.2018.06.028.

(31). Wang DH; Wang Z; Brenna JT Gas Chromatography Chemical Ionization Mass Spectrometry and Tandem Mass Spectrometry for Identification and Straightforward Quantification of Branched Chain Fatty Acids in Foods. J. Agric. Food Chem. 2020, 68 (17), 4973–4980. 10.1021/acs.jafc.0c01075. [PubMed: 32298092]

(32). Zirrolli JA; Murphy RC Low-Energy Tandem Mass Spectrometry of the Molecular Ion Derived from Fatty Acid Methyl Esters: A Novel Method for Analysis of Branched-Chain Fatty Acids. J. Am. Soc. Mass Spectrom. 1993, 4 (3), 223–229. 10.1016/1044-0305(93)85085-C. [PubMed: 24234851]

(33). Svetashev VI; Kharlamenko VI Fatty Acids of Abyssal Echinodermata, the Sea Star Eremicaster Vicinus and the Sea Urchin Kamptosoma Abyssale: A New Polyunsaturated Fatty Acid Detected, 22:6(n-2). Lipids 2020, 55 (3), 291–296. 10.1002/lipd.12227. [PubMed: 32101331]

(34). Christie WW Gas Chromatography-Mass Spectrometry Methods for Structural Analysis of Fatty Acids. Lipids 1998, 33 (4), 343–353. 10.1007/s11745-998-0214-x. [PubMed: 9590621]

(35). Harvey DJ Picolinyl Esters as Derivatives for the Structural Determination of Long Chain Branched and Unsaturated Fatty Acids. Biomed. Mass Spectrom. 1982, 9 (1), 33–38. 10.1002/bms.1200090107.

(36). Han X; Gross RW Structural Determination of Picomole Amounts of Phospholipids via Electrospray Ionization Tandem Mass Spectrometry. J. Am. Soc. Mass Spectrom. 1995, 6 (12), 1202–1210. 10.1016/1044-0305(95)00568-4. [PubMed: 24214071]

(37). Pulfer M; Murphy RC Electrospray Mass Spectrometry of Phospholipids. Mass Spectrom. Rev. 2003, 22 (5), 332–364. 10.1002/mas.10061. [PubMed: 12949918]

(38). Gross ML Charge-Remote Fragmentation: An Account of Research on Mechanisms and Applications. Int. J. Mass Spectrom. 2000, 200 (1), 611–624. 10.1016/S1387-3806(00)00372-9.

(39). Kerwin JL; Wiens AM; Ericsson LH Identification of Fatty Acids by Electrospray Mass Spectrometry and Tandem Mass Spectrometry. J. Mass Spectrom. 1996, 31 (2), 184–192. 10.1002/(SICI)1096-9888(199602)31:2<184::AID-JMS283>3.0.CO;2-2. [PubMed: 8799272]

(40). Narreddula VR; Boase NR; Ailuri R; Marshall DL; Poad BLJ; Kelso MJ; Trevitt AJ; Mitchell TW; Blanksby SJ Introduction of a Fixed-Charge, Photolabile Derivative for Enhanced Structural Elucidation of Fatty Acids. Anal. Chem. 2019, 91 (15), 9901–9909. 10.1021/acs.analchem.9b01566. [PubMed: 31298837]

(41). Narreddula VR; Sadowski P; Boase NRB; Marshall DL; Poad BLJ; Trevitt AJ; Mitchell TW; Blanksby SJ Structural Elucidation of Hydroxy Fatty Acids by Photodissociation Mass Spectrometry with Photolabile Derivatives. Rapid Commun. Mass Spectrom. 2020, 34 (9), e8741. 10.1002/rcm.8741. [PubMed: 32012356]

(42). Pham HT; Trevitt AJ; Mitchell TW; Blanksby SJ Rapid Differentiation of Isomeric Lipids by Photodissociation Mass Spectrometry of Fatty Acid Derivatives. Rapid Commun. Mass Spectrom. 2013, 27 (7), 805–815. 10.1002/rcm.6503. [PubMed: 23495027]

(43). Blevins MS; James VK; Herrera CM; Purcell AB; Trent MS; Brodbelt JS Unsaturation Elements and Other Modifications of Phospholipids in Bacteria: New Insight from Ultraviolet Photodissociation Mass Spectrometry. Anal. Chem. 2020, 92 (13), 9146–9155. 10.1021/acs.analchem.0c01449. [PubMed: 32479092]

(44). Narreddula VR; McKinnon BI; Marlton SJP; Marshall DL; Boase NRB; Poad BLJ; Trevitt AJ; Mitchell TW; Blanksby SJ Next-Generation Derivatization Reagents Optimized for Enhanced Product Ion Formation in Photodissociation-Mass Spectrometry of Fatty Acids. The Analyst 2021, 146 (1), 156–169. 10.1039/D0AN01840F. [PubMed: 33125008]

(45). Bollinger JG; Thompson W; Lai Y; Oslund RC; Hallstrand TS; Sadilek M; Turecek F; Gelb MH Improved Sensitivity Mass Spectrometric Detection of Eicosanoids by Charge Reversal Derivatization. Anal. Chem. 2010, 82 (16), 6790–6796. 10.1021/ac100720p. [PubMed: 20704368]

(46). Lin Q; Li P; Jian R; Xia Y Localization of Intrachain Modifications in Bacterial Lipids Via Radical-Directed Dissociation. J. Am. Soc. Mass Spectrom. 2022, 33 (4), 714–721. 10.1021/jasms.2c00011. [PubMed: 35195000]

(47). Zhao X; Wu G; Zhang W; Dong M; Xia Y Resolving Modifications on Sphingoid Base and N-Acyl Chain of Sphingomyelin Lipids in Complex Lipid Extracts. Anal. Chem. 2020, 92 (21), 14775–14782. 10.1021/acs.analchem.0c03502. [PubMed: 33052665]

(48). Zhao X; Xia Y Characterization of Fatty Acyl Modifications in Phosphatidylcholines and Lysophosphatidylcholines via Radical-Directed Dissociation. J. Am. Soc. Mass Spectrom. 2021, 32 (2), 560–568. 10.1021/jasms.0c00407. [PubMed: 33444004]

(49). Pham T, H. R, Julian R Characterization of Glycosphingolipid Epimers by Radical-Directed Dissociation Mass Spectrometry. Analyst 2016, 141 (4), 1273–1278. 10.1039/C5AN02383A. [PubMed: 26800360]

(50). Randolph CE; Foreman DJ; Betancourt SK; Blanksby SJ; McLuckey SA Gas-Phase Ion/Ion Reactions Involving Tris-Phenanthroline Alkaline Earth Metal Complexes as Charge Inversion Reagents for the Identification of Fatty Acids. Anal. Chem. 2018, 90 (21), 12861–12869. 10.1021/acs.analchem.8b03441. [PubMed: 30260210]

(51). Chao H-C; McLuckey SA Differentiation and Quantification of Diastereomeric Pairs of Glycosphingolipids Using Gas-Phase Ion Chemistry. Anal. Chem. 2020, 92 (19), 13387–13395. 10.1021/acs.analchem.0c02755. [PubMed: 32883073]

(52). Randolph CE; Blanksby SJ; McLuckey SA Toward Complete Structure Elucidation of Glycerophospholipids in the Gas Phase through Charge Inversion Ion/Ion Chemistry. Anal. Chem. 2020, 92 (1), 1219–1227. 10.1021/acs.analchem.9b04376. [PubMed: 31763816]

(53). Randolph CE; Shenault DM; Blanksby SJ; McLuckey SA Structural Elucidation of Ether Glycerophospholipids Using Gas-Phase Ion/Ion Charge Inversion Chemistry. J. Am. Soc. Mass Spectrom. 2020, 31 (5), 1093–1103. 10.1021/jasms.0c00025. [PubMed: 32251588]

(54). Randolph CE; Shenault DM; Blanksby SJ; McLuckey SA Localization of Carbon–Carbon Double Bond and Cyclopropane Sites in Cardiolipins via Gas-Phase Charge Inversion Reactions. J. Am. Soc. Mass Spectrom. 2021, 32 (2), 455–464. 10.1021/jasms.0c00348. [PubMed: 33370110]

(55). Chao H-C; McLuckey SA In-Depth Structural Characterization and Quantification of Cerebrosides and Glycosphingosines with Gas-Phase Ion Chemistry. Anal. Chem. 2021, 93 (19), 7332–7340. 10.1021/acs.analchem.1c01021. [PubMed: 33957046]

(56). Randolph CE; Foreman DJ; Blanksby SJ; McLuckey SA Generating Fatty Acid Profiles in the Gas Phase: Fatty Acid Identification and Relative Quantitation Using Ion/Ion Charge Inversion Chemistry. Anal. Chem. 2019, 91 (14), 9032–9040. 10.1021/acs.analchem.9b01333. [PubMed: 31199126]

(57). Randolph CE; Marshall DL; Blanksby SJ; McLuckey SA Charge-Switch Derivatization of Fatty Acid Esters of Hydroxy Fatty Acids via Gas-Phase Ion/Ion Reactions. Anal. Chim. Acta 2020, 1129, 31–39. 10.1016/j.aca.2020.07.005. [PubMed: 32891388]

(58). Liebisch G; Vizcaíno JA; Köfeler H; Trötzmüller M; Griffiths WJ; Schmitz G; Spener F; Wakelam MJO Shorthand Notation for Lipid Structures Derived from Mass Spectrometry. J. Lipid Res. 2013, 54 (6), 1523–1530. 10.1194/jlr.M033506. [PubMed: 23549332]

(59). Xia Y; Wu J; McLuckey SA; Londry FA; Hager JW Mutual Storage Mode Ion/Ion Reactions in a Hybrid Linear Ion Trap. J. Am. Soc. Mass Spectrom. 2005, 16 (1), 71–81. 10.1016/j.jasms.2004.09.017. [PubMed: 15653365]

(60). Xia Y; Liang X; McLuckey SA Pulsed Dual Electrospray Ionization for In/In Reactions. J. Am. Soc. Mass Spectrom. 2005, 16 (11), 1750–1756. 10.1016/j.jasms.2005.07.013. [PubMed: 16182558]

(61). Londry FA; Hager JW Mass Selective Axial Ion Ejection from a Linear Quadrupole Ion Trap. J. Am. Soc. Mass Spectrom. 2003, 14 (10), 1130–1147. 10.1016/S1044-0305(03)00446-X. [PubMed: 14530094]

(62). Hsu F-F; Turk J Electrospray Ionization/Tandem Quadrupole Mass Spectrometric Studies on Phosphatidylcholines: The Fragmentation Processes. J. Am. Soc. Mass Spectrom. 2003, 14 (4), 352–363. 10.1016/S1044-0305(03)00064-3. [PubMed: 12686482]

(63). Ekroos K; Ejsing CS; Bahr U; Karas M; Simons K; Shevchenko A Charting Molecular Composition of Phosphatidylcholines by Fatty Acid Scanning and Ion Trap MS3 Fragmentation. J. Lipid Res. 2003, 44 (11), 2181–2192. 10.1194/jlr.D300020-JLR200. [PubMed: 12923235]

(64). Huynh K; Barlow CK; Jayawardana KS; Weir JM; Mellett NA; Cinel M; Magliano DJ; Shaw JE; Drew BG; Meikle PJ High-Throughput Plasma Lipidomics: Detailed Mapping of the Associations with Cardiometabolic Risk Factors. Cell Chem. Biol. 2019, 26 (1), 71–84.e4. 10.1016/j.chembiol.2018.10.008. [PubMed: 30415965]

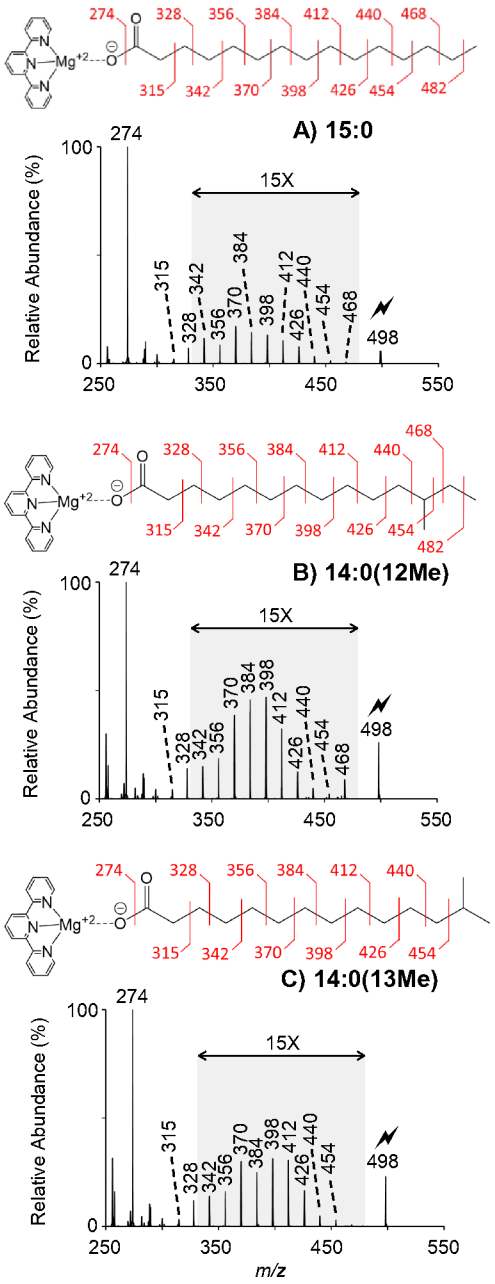

Figure 1.

Ion-trap CID of $[M - H + MgTerpy]^+$ derived from the gas phase ion/ion reaction of $[MgTerpy2]^{2+}$ with the $[M - H]^-$ anions, where M = **(A)** FA 15:0, **(B)** FA 14:0(12Me), and **(C)** FA 14:0(13Me).

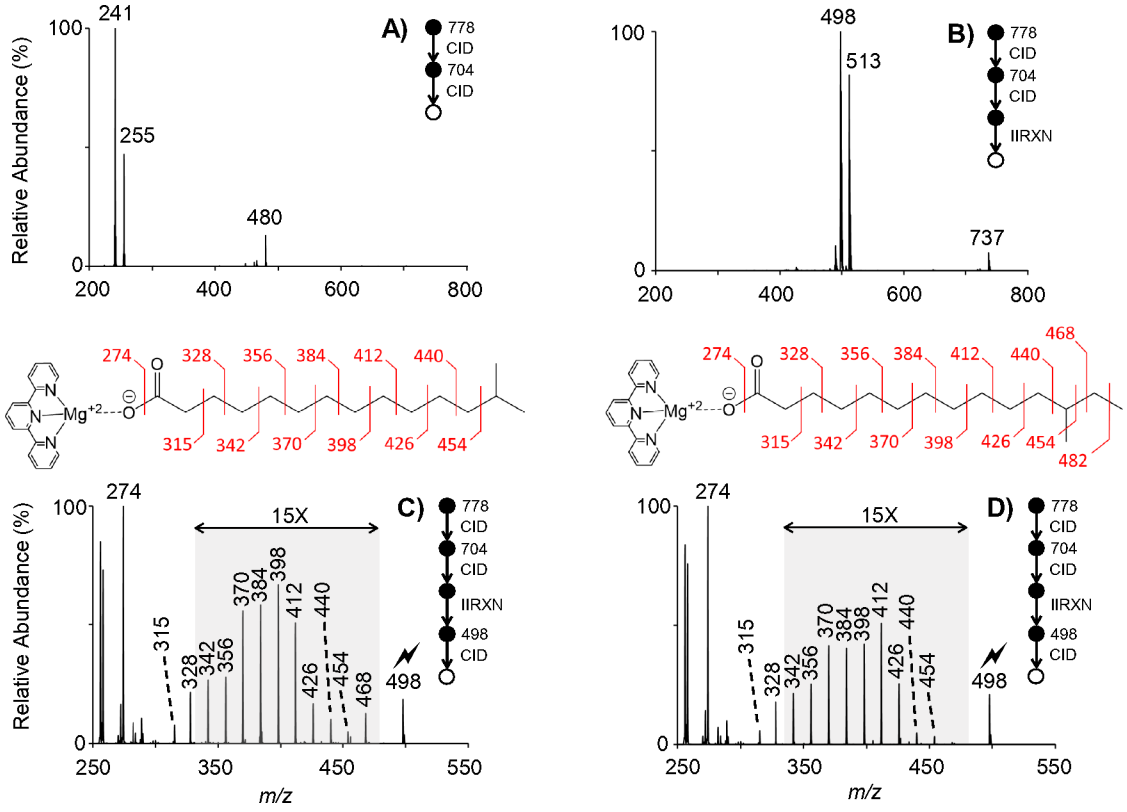

Figure 2.

Sequence of MS events used to interrogate the molecular structures of the phosphatidylcholine isomers, PC 16:0/14:0(12Me) and PC 16:0/14:0(13Me). **A)** Ion-trap CID spectrum of[PC 16:0/14:0(12Me) − CH_3]$^-$ (*mlz* 704). **B)** Charge inversion spectrum generated via the gas-phase ion/ion reaction between product ions generated from CID of the [PC − CH_3]$^-$ precursor ion as shown in **(A)** and [MgTerpy2]$^{2+}$ reagent dications. Ion-trap CID product ion spectrum following monoisotopic mass selection and collisional activation of the branched FA complex cation at *mlz* 498, derived from **C)** PC 16:0/14:0(12Me) and **D)** PC 16:0/14:0(13Me).

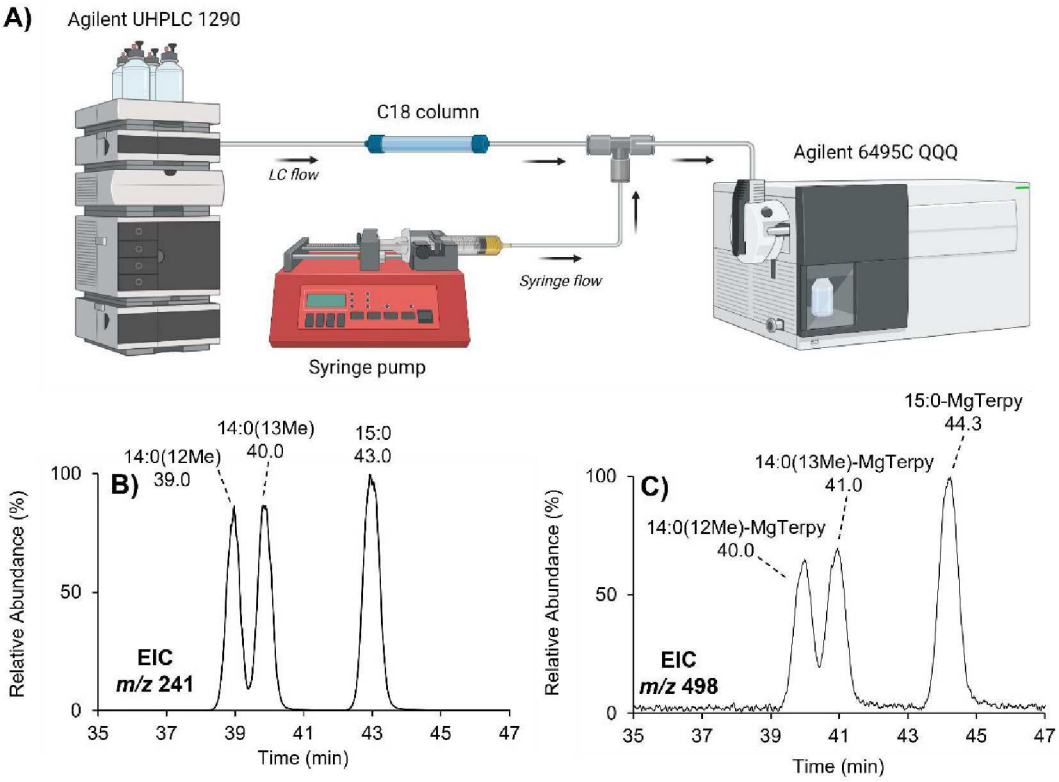

Figure 3.

A) Illustrative schematic of post-column charge switching LC-MS/MS method. **B)** EiC of *m/z* 241 without FA derivatization (*i.e.*, negative ion mode). **C)** EiC of *m/z* 498 with FA derivatization (*i.e.*, positive ion mode).

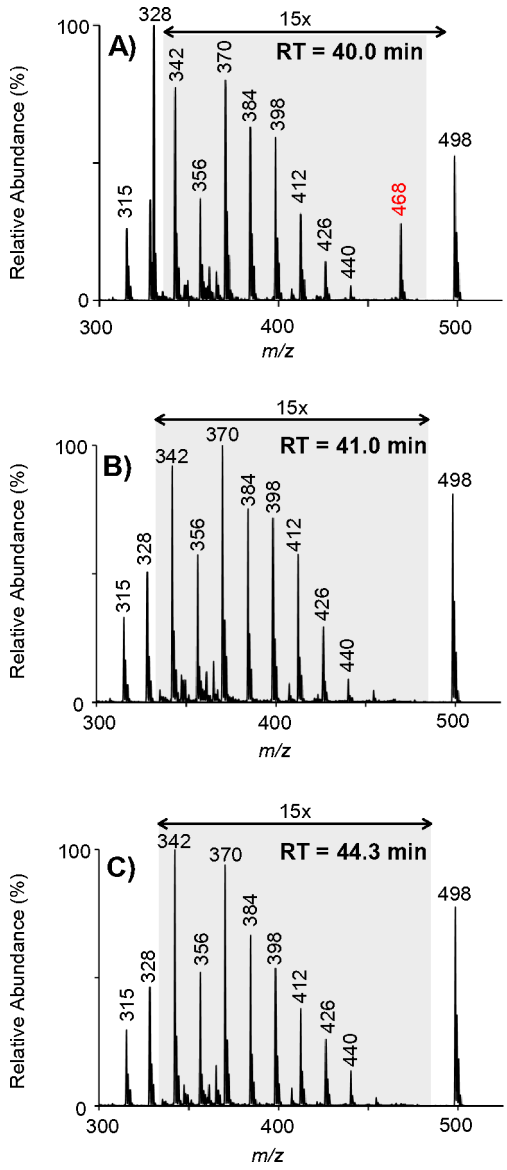

Figure 4.

LC MS/MS spectra of charge-switched **A)** FA 14:0(12Me), **B)** FA 14:0(13ME) and **C)** FA 15:0.

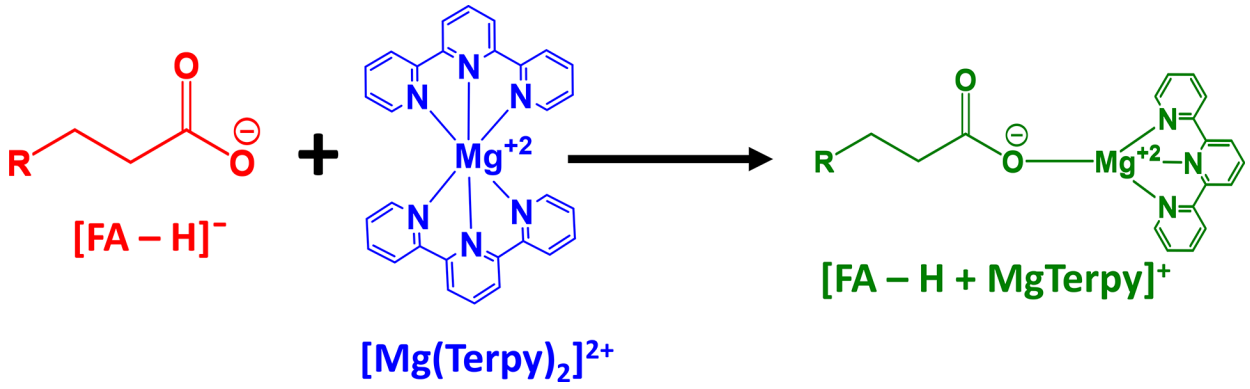

Scheme 1.

Generation of $[FA - H + MgTerpy]^+$ complex cations via ion/ion reaction of singly deprotonated FA anions and reagent bis-terpyridine magnesium dications.